FRC'98, Newcastle upon Tyne (UK)

THERMOMECHANICAL PROPERTIES OF WOVEN FABRIC COMPOSITES

R. Akkerman & R.S. de Vries
University of Twente

The in-plane thermo-elastic behaviour of woven fabric reinforced composites is analysed using a combination of published micromechanics and finite element techniques. The repetitive unit of an arbitrary woven fabric composite is divided into elements of which the thermo-elastic properties are determined using micromechanics. The properties of the repetitive unit are obtained using the finite element model. The presented model predicts the laminate stiffness and thermally induced forces and moments, from which the thermal expansion and bending coefficients and the residual deformations of the fabric laminate are derived. The theoretical results are validated by experiments on thermoplastic PEI-carbon and PPS-carbon 5H satin weave fabric laminates.

INTRODUCTION

Woven textile structures are often used as reinforcement in composite materials. Their ease of handling, low fabrication cost, good stability, balanced properties and excellent formability make the use of woven fabrics very attractive for structural applications in for example the automotive and aerospace industry. When using thermoplastics as a matrix material the products can be made by e.g. thermoforming, which enables a relatively high production rate compared to autoclave processes.

Due to hot processing of the laminates, the products contain internal stresses. These will affect the product strength and can cause undesired warpage. For reasons of dimensional accuracy and strength prediction of woven fabric composites it is important to understand the thermo-mechanical performance. In this, the complicated geometry of the fabric yarn plays an important role.

Several models have been developed to predict the in-plane thermo-elastic behaviour of various woven fabric structures. The engineering constants in load direction are modelled in [1,2,3] using convenient parallel-series arrangements of infinitesimal pieces. Vandeurzen and Verpoest [4,5] developed the combi-cell model that predicts the three dimensional elastic properties of fabric composites. This combi-cell consists of several micro cells between which either a uniform-strain or uniform-stress relation is used.

Here, we try to find a means for predicting the in-plane thermal and elastic constants and for an arbitrary weave and the resulting warpage due to residual stresses after processing, without assuming uniform strains or stresses throughout the laminate. Three levels of material structure are distinguished, a macro, meso and micro level. At micro level the elastic and thermal properties of the geometrically different elements of the repetitive unit of the fabric composite are determined using a two-dimensional model, similar to Naik and Shembekar [2,3]. At meso level the fabric pattern is taken into account and the element properties are linked using a finite element approach. At macro level the homogeneous properties and warpage of woven fabric composites are considered. This finite element formulation replaces the assumption of uniform strain or uniform stress within the fabric laminate. Although the presented model is confined to 5H-satin weave laminates, it can simply be used for all orthogonal fabric laminates.

MICRO LEVEL

In fig.*1*a the Representative Volume Element (RVE) that represents the repetitive pattern of a 5H satin weave fabric is shown. The Cartesian *xyz*-coordinate system as displayed in the figure is used as a reference, the warp and fill yarns correspond respectively with the *x* and *y* direction and the positive *z*-direction is directed downwards. The RVE contains five warp and fill yarns of equal width *a*. To examine the interlaced parts of the yarns the RVE is subdivided into 25 square elements, among which three geometrically different elements can be distinguished, these are shown in fig.1b and 2. The material of the warp and fill yarns is the same.

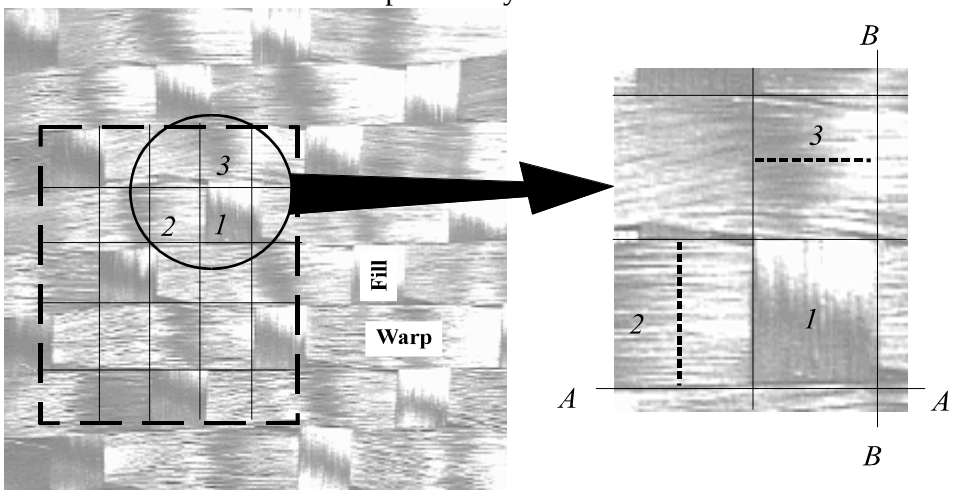

(a) (b)

1.(a) the unit cell of a 5H satin weave, the dotted region represents a repetitive unit cell magnification 5x, (b) the magnification of the three different elements (10×)

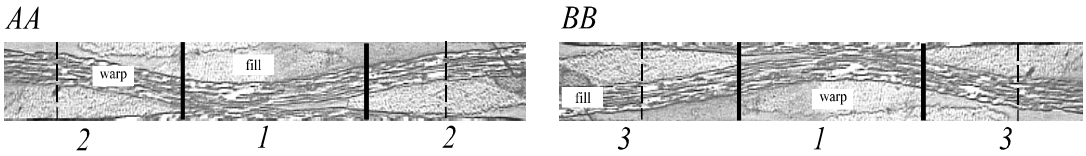

2. (a) the cross-section of fabric laminae, along line A-A of fig.1b. (b) the cross-section along line B-B. The numbers correspond with the element numbers of fig.1, magnification 10x

Shape functions

Similar to Naik and Shembekar [2,3] the boundaries of the warp and fill yarns of the three elements are defined as sinusoidal functions of *x* and *y*,

$$h_i(x,y) = c_i F_w(x) + d_i F_f(y) + h^k \qquad \textbf{(1)}$$

in which c_i and d_i are constants belonging to the shape function $h_i(x,y)$, the index *i* denotes the boundaries of the matrix or the yarns within a laminae, h^k is the coordinate of the midplane of the k^{th} laminae and the subscripts *f* and *w* denote respectively fill and warp. The geometry functions $F_w(x)$ and $F_f(y)$ are given by

$$F_i(x) = \begin{cases} -1 & x \in [0, a_{0i}] \\ \sin\left\{\left(x - \dfrac{a_i}{2}\right)\dfrac{p}{a_{ui}}\right\} & x \in [a_{0i}, \tfrac{1}{2}a_i] \end{cases} \quad \text{with } a_{0i} = \tfrac{1}{2}(a_i - a_{ui}), \; i = f, w \qquad \textbf{(2)}$$

Using these geometry functions, the planes subdividing the different layers can be defined by the yarn shape functions $h_i(x,y)$ for the different element types, as depicted in fig.3.

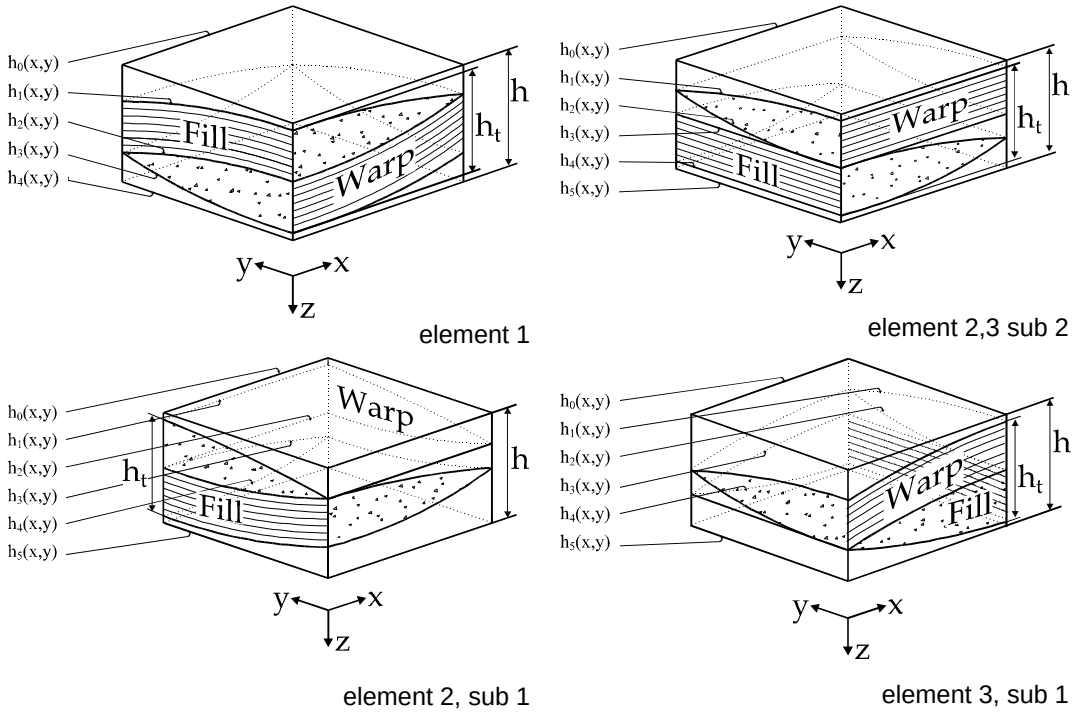

3. Yarn shape functions

Thermomechanical properties

The analysis of the mechanical properties is based on the assumption that the Classical Lamination Theory (CLT) [6] is applicable to each infinitesimal piece of the k^{th} laminae. The constitutive equations and the in-plane stiffness constants are given by:

$$\begin{Bmatrix} N_i \\ M_i \end{Bmatrix}^k = \begin{bmatrix} A_{ij}(x,y) & B_{ij}(x,y) \\ B_{ji}(x,y) & D_{ij}(x,y) \end{bmatrix}^k . \begin{Bmatrix} e_j^0 \\ k_j \end{Bmatrix} \qquad (\mathrm{i,j} = 1,2,6) \qquad \textbf{(3)}$$

where

$$\left(A_{ij}(x,y), B_{ij}(x,y), D_{ij}(x,y) \right)^k = \int_{h^k + \frac{h}{2}}^{h^k - \frac{h}{2}} \left(1, z, z^2\right) Q_{ij}^k \, dz \qquad \textbf{(4)}$$

in which Q^k_{ij} is the elastic stiffness matrix, z the height coordinate and h the laminae thickness. The stiffness matrices of the warp and fill yarns are a function of the local yarn angle, which is the first derivative of the yarn shape function:

$$q_x = \arctan \frac{\partial h(x,y)}{\partial x}, \; q_y = \arctan \frac{\partial h(x,y)}{\partial y} \qquad \textbf{(5)}$$

in which *h(x,y)* is the appropriate shape function of the undulated yarn. The stiffness matrix Q_{ij} is evaluated with respect to the global *xyz* coordinate system and is derived from the elastic constants in the principal material direction as follows [7]:

$$
\begin{aligned}
E_x(q) &= \left[l_q^{\,4} \,/ E_L + \left(1/G_{LT} - 2u_{LT}/E_L\right) l_q^{\,2} m_q^{\,2} + m_q^{\,4} \,/ E_T \right]^{-1} \\
E_y(q) &= E_T \\
n_{xy}(q) &= E_x(q) \left[l_q^{\,2} n_{LT} / E_L + m_q^{\,2} n_{TT} / E_T \right] \\
G_{xy}(q) &= \left[m_q^{\,2} / G_{TT} + l_q^{\,2} / G_{LT} \right]^{-1}
\end{aligned}
\qquad
\begin{aligned}
l_q &= \cos(q) \\
m_q &= \sin(q)
\end{aligned}
\qquad \textbf{(6)}
$$

Here, q is the local angle of the warp or fill yarn and E_L and E_T are the moduli in respectively the longitudinal and the transverse fibre direction. The elastic properties in principle directions of the impregnated yarns are obtained from fibre and matrix properties using the CCA model [8].

The average in-plane constants over the element area can now be obtained using the 2D WF Parallel/Parallel (PP) scheme or Series/Series (SS) scheme as described by Naik and Shembekar [2,3], assuming either a uniform strain (PP) or a uniform stress state (SS) in both directions

According to the CLT the thermally induced forces and moments are given by :

$$
\begin{Bmatrix} \mathrm{N_j} \\ \mathrm{M_j} \end{Bmatrix}^k = -\Delta T \begin{Bmatrix} \tilde{A}_j \\ \tilde{B}_j \end{Bmatrix}^k \qquad (j = 1,2,6) \qquad \textbf{(7)}
$$

in which

$$
\begin{aligned}
\left(\tilde{A}_j(x,y), \tilde{B}_j(x,y)\right)^k &= \int_{h^k}^{h^{k-1}} (1,z) q_j^k \, dz \qquad (j=1,2,6) \\
q_j^k &= Q_{ij}^k a_j^{\,k}(q) \\
a_x &= a_1 \cos^2(q) + a_2 \sin^2(q), \quad a_y = a_2, \quad a_{xy} = 0
\end{aligned}
\qquad \textbf{(8)}
$$

Here, a_j contains the thermal expansion coefficients with respect to the *xyz* coordinate system of the warp or fill yarn or the matrix material. For the warp and fill yarn these depend on the fibre volume fraction and are determined using the model of Schapery [9]. Straightforwardly the thermally induced forces and moments can be determined for the different (sub) elements.

MESO LEVEL

The CLT is based on the Kirchhoff plate theory, which assumes plane stress and zero transverse shear. For multilayered composite plates the strain profile is given by

$$
\{e(z)\} = \{e^0\} + z\{k\} \qquad \textbf{(9)}
$$

in which e^0 and k are respectively the strain and curvatures of the laminate geometric midplane. The stress profile follows automatically by multiplying equation (9) with the stiffness matrix Q_{ij}^k

$$
\{s(z)\} = [\mathrm{Q}]^k \{e(z)\} \qquad \textbf{(10)}
$$

Equations (9) and (10) are substituted in the equation for the minimum of virtual work, containing the volume integral of the element stiffnesses and displacements and the surface integral of the applied forces.

$$
d\Pi = \frac{1}{2} \int_A \int_h \left\{ de^0 + z\,dk \right\}^T \cdot \left\{ [\mathrm{Q}]^k \left\{ e^0 + z k \right\} \right\} dz\,dA - \int_\Gamma v_i t_i \, d\Gamma \equiv 0 \quad (\forall\, de \wedge dk) \qquad \textbf{(11)}
$$

in which $\delta\varepsilon^0$ and $\delta\kappa$ are the virtual strains and curvatures, n_i the displacements, t_i the tractions and G the boundary. Here, the body forces are assumed to be zero. In the finite element representation equation (11) is integrated over the element thickness, using for the midplane strains and curvatures:

$$\begin{aligned} \{de^0\} &= [B_h]\{d\mathrm{u}\} \quad , \quad \{e^0\} = [B_h]\{\mathrm{u}\} \\ \{dk\} &= [B_b]\{dj\} \quad , \quad \{k\} = [B_b]\{j\} \end{aligned} \tag{12}$$

where B_h and B_b contain the first derivatives of the finite element trial functions of respectively the element displacements, $\{u\}$, and rotations, $\{j\}$. $\{\delta u\}$ and $\{\delta j\}$ are respectively the virtual displacements and rotations. This then results in the finite element formulation, symbolically written as:

$$\int_A \begin{bmatrix} B_h & 0 \\ 0 & B_b \end{bmatrix}^T \begin{bmatrix} A_{ij} & B_{ij} \\ B_{ij} & D_{ij} \end{bmatrix}^k \begin{bmatrix} B_h & 0 \\ 0 & B_b \end{bmatrix} dA \begin{Bmatrix} u \\ j \end{Bmatrix} = \{F\}^k \tag{13}$$

where $\{F\}$ contains the prescribed nodal forces. To solve the finite element problem the Discrete Kirchhoff Triangle (DKT) element with three integration points as described by Carleer [10] and Batoz [11] is used.

MACRO LEVEL

The FE-model replaces the assumption of a homogeneous strain or stress state within the RVE. However, when considering the response to a macroscopically homogeneous stress state, the local deformations of the elements must represent a macroscopically homogeneous strain state. The deformations on the sides of the RVE model are restricted by a condition of periodicity. To this end a linear relation is prescribed between the difference in nodal displacements and rotations of the opposite RVE sides and the nodal displacements and rotations of the RVE corner nodes. The actual constraint equations are given below.

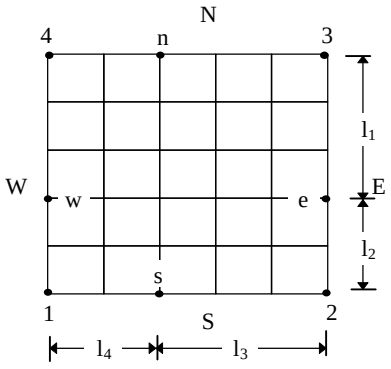

4. RVE model of a 5H satin weave

$$\begin{aligned} U_e - U_w &= \frac{l_2}{l_1 + l_2}\Delta U_N + \frac{l_1}{l_1 + l_2}\Delta U_S \\ \Delta U_N &= U_3 - U_4 \\ \Delta U_S &= U_2 - U_1 \end{aligned} \tag{14}$$

and

$$\begin{aligned} U_n - U_s &= \frac{l_4}{l_3 + l_4}\Delta U_E + \frac{l_3}{l_3 + l_4}\Delta U_W \\ \Delta U_E &= U_3 - U_2 \\ \Delta U_W &= U_4 - U_1 \end{aligned} \tag{15}$$

Now, any macroscopically linear displacement or rotation field can be described by only applying loads on the corner nodes of the RVE model. The degrees of freedom and the reaction forces of these four corner nodes are used to determine the homogenised stress and strain state and thus the homogenised orthotropic stiffnesses.

The homogenised thermal properties of the woven fabric composite are determined by prestressing the elements with the thermally induced element forces and moments, equation (7). The FE model (again subjected to the condition of periodicity) then gives the resulting nodal displacements and rotations of the four corner nodes. These, in turn,

lead to the homogenised thermal expansion and bending coefficients of the corresponding orthotropic continuum.

EXPERIMENTAL WORK

In order to verify the model, single layered woven fabric composites have been moulded. The non symmetric structure leads to significantly curved plates. The deflections have been compared to the model predictions. As large deformations occur, a non-linear theory must be used in addition to the predictive model for the thermo-elastic constants, as in [12,13].

Experiments were performed on polyetherimide (PEI) and polyphenylenesulfide (PPS) samples reinforced with respectively 46 and 45 volume percent T-300 carbon fibres. Samples of 250x250 mm^2 were made by compression moulding in an enclosed mould. The PEI and PPS samples were produced at respectively 325 °C and 310 °C and both at 8 bar pressure for a duration of 30 minutes. The cooling rate for both samples was 5 °C/min. Fibre alignment after compression moulding was within 2 degrees correct. The maximum misalignment of 2 degrees fibre angle does not cause substantial errors in the calculations. The fabric thickness, h_t, and the undulated length, a_{uw} and a_{uf}, of the warp and fill yarn and the yarn with a_w and a_f were determined from microscopic pictures.

Thermal expansion coefficients a_w and a_f were measured by mounting strain gauges in warp and fill direction on both sides of the specimens to exclude possible bending. The specimens were heated up to 80 °C and cooled down in approximately 3 hours monitoring the strain development. In total four specimens, two of each material, were used in the experiments. To obtain more reliable data each specimen was measured three times.

For the measurement of residual deformations two 1-layer samples of both PEI and PPS were used. Three specimens were cut from each sample, thus a total 12 specimens were measured, their average dimensions are given in table I. The curvatures in length and width direction of the sample were determined by measuring the coordinates of 600 points at the surface of the specimens. All specimens were measured within a few hours after processing at temperature $T << T_g$, therefore creep of the specimens is considered to be irrelevant.

		PPS/T-300 Carbon		PEI/T-300 Carbon	
		Average	Range	Average	Range
Thickness	mm	0.30	0.28-0.30	0.32	0.31-0.33
Length	mm	90	89-91	90.0	89-91
Width	mm	29.6	30.1-29.5	29.6	29.5-29.7
V_f	%	46		45	

I. Dimensions of used specimens

RESULTS AND DISCUSSION

In table III and IV the measured and predicted thermal expansion coefficients of respectively the PEI/Carbon and the PPS/Carbon specimens are tabulated. Since the results of the experiments showed a considerable scatter, the average of the different measurements is taken. No significant difference was found between the measured expansion coefficient in warp and fill direction. Comparison of the experimental results and predicted values shows that the parallel model gives a good approximation of the thermal expansion coefficient for both materials. The series model predicts a considerable higher thermal expansion coefficient due to the underestimation of the material stiffnesses.

The curvatures of the laminate that are present after hot processing are the results of stresses that build up in the material during solidification of the laminate. A viscous-elastic behaviour is assumed, in which stresses above T_g relax immediately and below T_g the material is considered elastic. Both the amorphous PEI and the semi-crystalline PPS show no secondary relaxations below the glass transition temperature [14, 15], which supports the assumption of elasticity. Therefore, in the calculations the temperature interval, ΔT, between the glass-transition and the room temperature is used to predict the residual curvatures for both materials.

In table III and IV the measured and predicted curvatures in respectively the length and the width direction of the specimens are tabulated. The predicted values of the parallel model in the length direction (κ_x) are a good approximation of the experimentally determined curvatures. The predicted curvatures in the width direction (κ_y) deviate from the experimental values, which showed significant scatter as the absolute height difference in width direction is small compared to the measurement accuracy. The series model predicts for both the PEI/Carbon and PPS/Carbon laminates curvatures deviating considerably from the experimentally found values. Since the modelled thermal forces and moments are the same for the parallel and series model this difference is due to an underestimation of the laminate stiffnesses.

Finally, the relevance of the presented model can be showed by comparing the results with the calculated thermal expansion coefficients and residual curvatures under the assumption of a uniform strain within the RVE. The RVE stiffnesses and thermal forces and moments become then the average of the element stiffnesses and element thermal forces and moments. In the first row of table III and IV these average values are tabulated. Compared to the presented model a higher laminate stiffness is found when a uniform state of strain is assumed. The thermal forces and moments only show small differences. Consequently the residual curvatures of the laminate are significantly larger in the length and smaller in the width direction when a uniform strain is assumed. Considering the thermal expansion coefficients no significant difference is found.

Material	E_L GPa	E_T GPa	G_{LT} GPa	G_{TT} GPa	ν_{LT} -	α_1 10^{-6} °C^{-1}	α_2 10^{-6} °C^{-1}	ρ g/cm^3	T_g °C	T_c °C
T-300* carbon	231.0	40.0	24.0	14.4	0.26	-0.5	5.6	1.76	-	-
PPS matrix	4.4	4.4	1.62	1.62	0.37	51	51	1.35	88	130
PEI matrix	2.9	2.9	1.07	1.07	0.35	56	56	1.27	217	-

*II. Elastic and thermal properties of fibres and matrix material, * the properties of T-300 are found in literature [16]. The remaining properties have been determined by own measurements.*

PEI/T-300	κ_x m^{-1}	κ_y m^{-1}	α_w 10^{-6} °C $^{-1}$
Average stiffness	-9.5	0.7	4.5
Parallel	-11.5	0.5	4.0
Series	-15.2	0.4	6.6
Experimental	-11.0	1.2	4.3

III. Comparison of the experimental and predicted values of PEI/T-300 Carbon laminae, V_f=46%, a_w=a_f=1.5 mm, a_{uw}=a_{uf}=1.5 mm, h_t=h= 0.32mm, DT=197°C

PPS/T-300	κ_x m^{-1}	κ_y m^{-1}	α_w 10^{-6} °C $^{-1}$
Average stiffness	-2.2	2.2	4.5
Parallel	-2.8	1.9	4.5
Series	-4.4	1.3	6.8
Experimental	-3.0	1.4	3.9

IV. Comparison of the experimental and predicted values of PPS/T-300 Carbon laminae, V_f=45%, a_w=a_f=1.5 mm, a_{uw}=a_{uf}=1.5 mm, h_t=h= 0.30 mm, DT=68°C

CONCLUSION

The presented model to determine the thermo-elastic properties and warpage of woven fabric laminate gives a good correlation with experimental results when a uniform state of element strain is used. In case a uniform state of element stress is assumed the laminate stiffnesses are underestimated. The use of a FE formulation is results in closer bounds for the thermo-elastic properties of woven fabric laminates than the use of a uniform stress or strain state within the laminate.

ACKNOWLEDGEMENTS

The authors thank W.H.M. van Dreumel of Ten Cate Advanced Composites bv for his support and providing the necessary materials.

REFERENCES

1. T.W. Chou & T. Ishikawa, *Textile structural composites*, Amsterdam, Elsevier Science Publishers, 1991.
2. N.K. Naik & P.S. Shembekar, 'Elastic Behaviour of Woven Fabric Composites: I-Lamina Analysis', *J. Comp. Mat.*, 1992, **26** 2196-2225.
3. N.K. Naik & P.S. Shembekar, 'Elastic Behaviour of Woven Fabric Composites: II-Laminate Analysis', *J. Comp. Mat.*, 1992, **26** 2227-2246.
4. P. V&eurzen, J. Ivens & I. Verpoest, 'A Three Dimensional Micro Mechanical Analysis of Woven Fabric Composites: I. Geometric Analysis', Comp. Sci. Tech., 1996 **56** 1303-1315
5. P. Vandeurzen, J. Ivens & I. Verpoest, 'A Three Dimensional Micro Mechanical Analysis of Woven Fabric Composites: II. Elastic Analysis', *Comp. Sci. Tech.*, 1996 **56** 1317-1327
6. P.C. Powell, *Engineering with Fibre-Polymer Laminates*, London, Chapman & Hall, 1994,
7. P.F. Falzon & I. Herzberg, 'Effects of Compaction on the Stiffness and Strength of Plain Weave Fabric RTM Composites', *J. Comp. Mat.*, 1996 **30** 1211-1247.
8. Z. Hashin, 'Analysis of Composite Materials', *J. App. Mech.*, 1983 **50** 481
9. R.A. Schapery, Thermal Expansion Coefficients of Composite Materials based on Energy Principles, *J. Comp. Mat.*, 1975 **2** 380-404.
10. B.D. Carleer, *Finite element analysis of deep drawing*, PhD thesis, University of Twente, 1997.
11. J.L. Batoz, 'A Study of Three-Node Triangular Plate Bending Elements', *Int. J. Num. Met. Eng.*, 1908 **15** 1771-1812.
12. L.J.B. Peeters & L. Warnet, 'Thermally Induced Shapes of Unsymmetric Laminates', *J. Comp. Mat.*, 1996 **30** 603-626.
13. M.W. Hyer, 'Calculations of the Room Temperature Shapes of Unsymmetric Laminates', *J. Comp. Mat.*, 1981 **15** 318-340.
14. M.P.I.M. Eijpe & P.C. Powell, 'A Modified Layer Removal Analysis for the Determination of Internal Stresses in Polymer Composites, *J. Therm. Comp. Mat.*, 1997 **10** 334-352.
15. M. Chen-Chi & Hung-Chung Hsia, 'The development of thermal, reological and morphological properties of poly(phenylenesulfide) resin and composites', *Antec '86*, Soc. of Plastics Engineers, 1986.
16. R. Pandy & H.T. Hahn, 'A Micro Mechanic Model for 2D Fabrics', *proceedings of the American society for composites*, Lancaster PA, USA, 1992.